actuators

MDPI

Article

Development of Electro-Mechanical Actuator for Wheel Steering of Railway Vehicles

Hyun Moo Hur [1,*], Jung Won Seo [1], Kyung Ho Moon [1] and Jong Hyun Choi [2]

[1] Korea Railroad Research Institute, Uiwang-si 16105, Gyeonggi-do, Republic of Korea; jwseo@krri.re.kr (J.W.S.); khmoon@krri.re.kr (K.H.M.)
[2] Dodam Corporation, Hwaseong-si 18624, Gyeonggi-do, Republic of Korea; jhchoi@dodamtop.co.kr
* Correspondence: hmhur@krri.re.kr

Abstract: We developed an electro-mechanical actuator for use as a steering device for railway vehicles. The specifications for a 50 kN-class electro-mechanical actuator capable of steering control for a sharp of a railway radius curve of up to 250 m, and with Direct Drive motor (DD motor) specifications, were derived as a power source to drive it. The DD motor and an electric mechanical steering actuator equipped with it were designed and a prototype was manufactured. As a result of testing laboratory tests on motor and actuator prototypes, all performance requirements were satisfied. We conducted a field test on the actuator prototype by installing it on a railway vehicle to verify the steering angle performance. The steering action of the actuator worked well when running in curved sections, and the steering angles measured for each curve were in line with the target steering angles. The mean error between the target steering angle and the measured steering angle was only 3.4%, indicating that the wheel steering action of the developed steering system was working very well. Therefore, the developed electro-mechanical actuator is expected to be fully utilized as a steering device for railway vehicles by meeting all the performance requirements of the steering system.

Keywords: steering system; electro-mechanical actuator; railway vehicle; curved section

check for updates

Citation: Hur, H.M.; Seo, J.W.; Moon, K.H.; Choi, J.H. Development of Electro-Mechanical Actuator for Wheel Steering of Railway Vehicles. *Actuators* **2024**, *13*, 460. https://doi.org/10.3390/act13110460

Academic Editors: Seongjin Yim and Kanghyun Nam

Received: 12 October 2024
Revised: 11 November 2024
Accepted: 13 November 2024
Published: 15 November 2024

Copyright: © 2024 by the authors. Licensee MDPI, Basel, Switzerland. This article is an open access article distributed under the terms and conditions of the Creative Commons Attribution (CC BY) license (https://creativecommons.org/licenses/by/4.0/).

1. Introduction

Automobiles are equipped with a steering system when driving on curved sections, so they can smoothly pass through the curved section by steering the wheels. But railway vehicles running on fixed tracks are not equipped with steering systems. As a result, when running on curved sections, the wheels of railway vehicles are not steered, generating unnecessary forces between the wheels and the rails in the direction of travel. This leads to severe wear on the wheels and rails, as well as generating noise. These issues ultimately affect passenger comfort and increase maintenance costs for the railway operator.

To address these problems, active steering technology is being researched for application to improve the steering performance of railway vehicles [1–5]. In the early stages of steering technology research, theoretical studies were primarily conducted on control concepts, strategies, and technologies for active steering. Recently, steering systems have been developed and installed on railway vehicles, with performance testing conducted on a test track.

T. Michálek studied the steering performance of an active yaw damper-type active steering device with an electro-hydraulic actuator [6]. Y. Umehara developed an electro-hydraulic active steering device and confirmed a reduction in lateral forces on the wheels by steering wheels in curved sections during test operations [7]. Additionally, M. Suzuki also developed a pneumatic active steering system and attempted to apply it to railway vehicles [8]. But the electro-hydraulic steering system requires auxiliary devices such as hydraulic power units and hydraulic piping to generate hydraulic pressure, making it

inconvenient to apply to railway vehicles due to restrictions on installation space and maintenance problems. On the other hand, pneumatic steering systems use the air pressure from the main compressor of the railway vehicle, making them more practical since they do not require additional devices. But the characteristic of pneumatic control limits the ability to control precise and fast movements.

Therefore, in accordance with the trend in the electrification of mobility, this paper developed an electro-mechanical steering system that is easy to install in a railway vehicle because it has excellent control performance and does not require an auxiliary device. This is the world's first attempt at a steering system for a railway vehicle. We derived development specifications for railway vehicle applications and designed an electro-mechanical steering system to meet those specifications. A prototype of the steering system was manufactured, and performance tests were carried out using a test bench to verify its compliance with the design specifications. And, finally, the steering angle performance was tested by conducting a field test applied to railway vehicles. This paper details the results of that research.

2. Electro-Mechanical Actuator Design

2.1. Development Specifications

In order for a railway vehicle to drive ideally when passing through a curved section, the wheelset should be aligned in a radial position in line with the center of the curve radius, as shown in Figure 1, which ensures that the attack angle between the wheels and the rail is '0', allowing the curve to be passed smoothly. In the radial steering position, steering control for ideal curve running, the target steering angle (δ_{target}) formed between the two axes of the bogie, which is the driving device of the railway vehicle, is given by the expression $\delta_{target} = 2d/R$, based on the geometric relationship in Figure 1, where 2d is the wheel base and R is the radius of the curve [9].

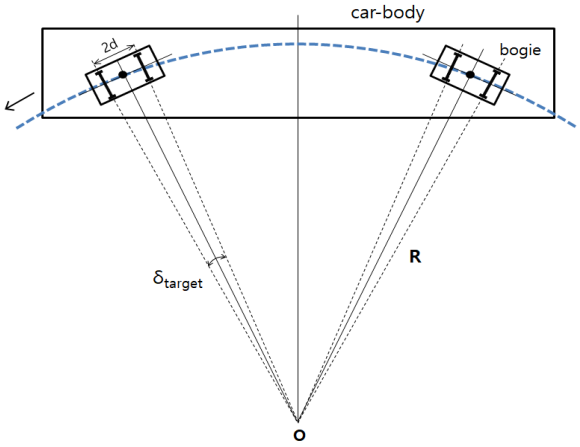


Figure 1. Radial steering position.

A steering action needs to be taken to achieve the steering angle by spreading the outer wheels of the curve and pulling the inner wheels using a steering actuator, as illustrated in Figure 2. Here, if the stroke of the steering actuator is Δ, the steering angle δ_{act} formed by the steering device is expressed as $\delta_{act} = 4\Delta/L$, based on the geometric relationship, where L is the distance between the outer and inner steering actuators. Therefore, for the development of electro-mechanical actuators to be applied to steering systems, performance objectives such as the actuator's force, stroke, and reaction speed have been derived.

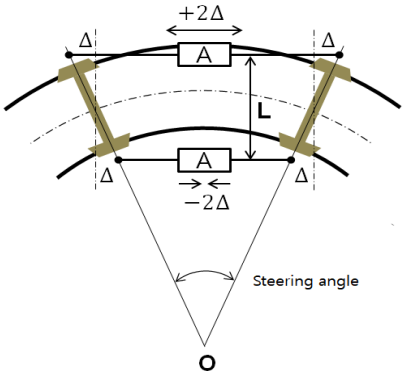


Figure 2. Wheelset steering motion.

The specifications of the steering system, intended for installation on a subway train that operate on urban railroad sections with many curves, were set at a level that enables smooth steering on sharp curves with a 250 m (R250) radius on the railway line.

First, the target steering angle for the operation in the R250 curve is 0.48 deg, given the curve radius (R) of 250 m and the wheelbase (2d) of the bogie, which is 2.1 m. The target steering angle, when translated into the actuator stroke (Δ), given the distance (L) of 2100 mm between the outer and inner steering actuators, as shown in Figure 2, will be equivalent to 4.41 mm.

A multi-body dynamic simulation was carried out to estimate the maximum actuation force required by the actuator to control the steering when passing through a curve. The simulation showed that the maximum steering force generated by the steering actuator was 46.5 kN [10]. Additionally, to derive specifications for the actuator's response time, the passing time for an urban railway vehicle to pass through a curved section when running on a commercial line was measured. As a result, the minimum transit time was 5.9 s, as shown in Figure 3. At this time, if the curve is assumed to be half the wavelength of the sine wave, the wavelength is 11.8 s, which is equivalent to 0.17 Hz when converted to frequency.

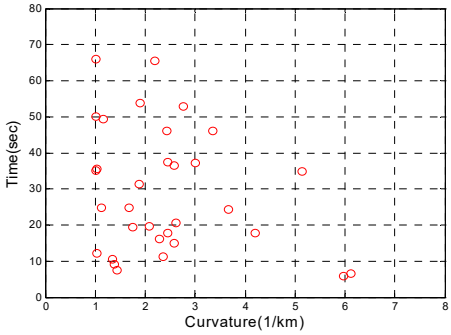


Figure 3. The results of measured passing time through the curved sections.

All the details explained above suggest that a stroke of 4.41 mm, a steering force of 46.5 kN, and a response frequency of 0.17 Hz or higher are required as minimum conditions for the smooth operation of the steering actuator. Therefore, since the performance of the future electro-mechanical actuator must exceed these minimum conditions, we set the specifications as shown in Table 1, taking into account mechanical errors in mounting the railroad vehicle and allowing a margin for stable performance.

Table 1. Basic required performance for development steering actuator.

Parameter	Specification
Actuator type	electro-mechanical
Force	above 50,000 N
Stroke	above ±5.5 mm
Response	above 0.3 Hz

Figure 4 shows the steering angle performance that the steering device to be developed can implement when applying the steering actuator specifications as shown in Table 1, and controlling the radial steering position steering. The target steering angle δ_{target} increases as the radius of the curve (R) decreases according to the steering angle calculation formula $\delta_{target} = 2d/R$ [9]. For the steering system to be developed, the stroke of the steering link is limited to 5.5 mm due to the limitation of the spring displacement of the primary suspension system connected to the steering link. Therefore, the steering angle that the steering actuator can attain from the geometric relationship in Figure 2 is limited to 0.5 degrees, which corresponds to the target steering angle for passing a curve with a radius of 240 m. Therefore, on a sharp curve smaller than a curved radius 240, the steering angle that the designed steering device may implement is limited to 0.5 deg.

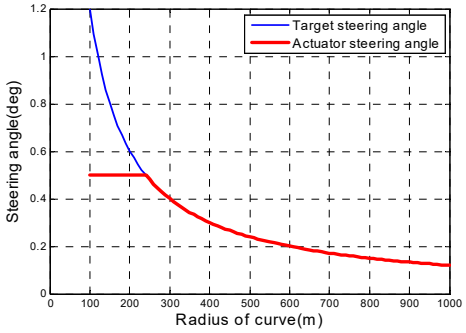
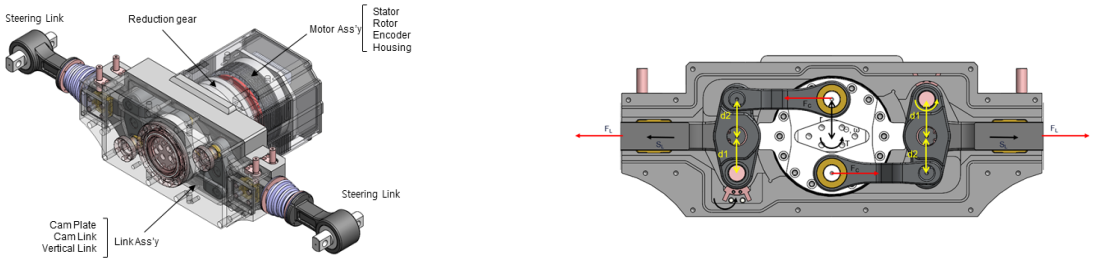


Figure 4. Steering angle performance of the development steering system.

2.2. Actuator Designs

Reflecting the specifications and requirements for the manufacture of steering actuators, an electro-mechanical actuator is designed. Figure 5 shows the proposed actuator design.



(**a**) (**b**)

Figure 5. Design of the electro-mechanical actuator; (**a**) 3D model; (**b**) link mechanism.

A Direct Drive motor (DD motor) of the Permanent Magnet Synchronous Motor type was chosen as the power source, and the rotational torque of the motor is amplified by a factor of N through a reduction gear. In front of the reduction gear, a mechanism consisting of a cam and a linkage is installed to convert the rotation angle (θ_M) of the motor into a linear displacement (s_L) of the steering link.

Equations (1) and (2) are expressions for the motor rotation angle and rotation speed. Equation (3) represents the rotation angle of the cam, and Equation (4) represents the displacement of the steering link. And Equation (5) represents the torque of the motor. Table 2 shows the parameters of the actuator.

$$\theta_M = \theta_{max} \times \sin(2\pi ft) \quad (1)$$

$$\omega_M = 2\pi ft \times \theta_{max} \times \cos(2\pi ft) \quad (2)$$

$$\theta_C = 1/N \times \theta_{max} \times \sin(2\pi ft) \quad (3)$$

$$s_L = R_L \times r/N \times \theta_{max} \times \sin(2\pi ft) \quad (4)$$

$$T_M = 2r \times F_L \times R_L/N \quad (5)$$

Table 2. Parameters of the actuator.

Parameter	Symbol	Spec.
DD motor rotation angle	θ_M	
DD motor rotation speed	ω_M	
DD motor torque	T_M	
Operating frequency	f	0.3 Hz
Reduction ratio	N	100
Cam rotation angle	θ_C	
Cam torque	T_C	
Displacement of cam link	s_{CL}	
Force of cam link	F_{CL}	
Distance between cam center and horizontal lever	r	55 mm
Ratio of link lever (R_L = d1/(d1 + d2))	R_L	1/2
Displacement of steering link	s_L	5.5 mm
Force of steering link	F_L	50,000 N

If the target specification, 5.5 mm is applied to the maximum displacement of the steering link in Equation (4), the maximum rotational angle of the motor (θ_{max}) is 3.184 rotation, and the angle is 20.0 rad.

Here, the motor speed is 6.0 rev/s by Equation (2), and it is 360 rpm if expressed in revolutions per minute. In addition, when the target steering force of 50,000 N and the reduction ratio of 100 are substituted into Equation (5), the driving torque of the motor becomes 27.5 Nm. Here, assuming an efficiency of the reduction gear of about 80%, the motor torque specification is approximately 35 Nm.

Figure 6 shows the configuration of the motor. The stator is arranged with alternating U-V-W coils with a phase angle of 120 °C, while the rotor has alternating permanent magnets with N and S poles. The absolute encoder, to detect the rotor's rotation angle, was used to measure the motor's rotation angle. The core of the stator is laminated with 0.5 mm thick electromagnetic steel sheets to reduce eddy current losses, and enameled copper windings of heat resistance class H (with a heat resistance temperature of 180 °C) are inserted into each core tooth. In addition, neodymium series (N45M) magnets with high magnetic flux density are applied to the permanent magnets of the rotor.

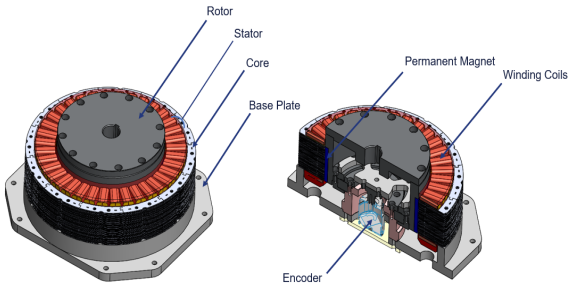


Figure 6. Configuration of DD motor.

Electromagnetic analysis was conducted to evaluate the torque performance of the designed DD motor using a finite element model, as shown in Figure 7. The geometry of the model for electromagnetic analysis is illustrated in Figure 7, while the structure and physical properties of the model are presented in Table 3. Figure 7 shows the finite element model for electromagnetic analysis. The electromagnetic analysis was conducted to examine the changes in continuous torque due to the rotation of the rotor and the variations in torque resulting from an increase in applied current.

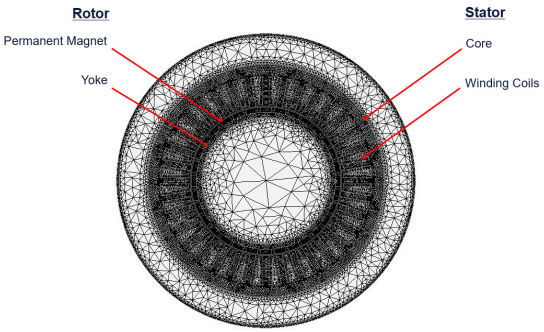


Figure 7. The 2D FE mesh of the DD motor.

Table 3. Specification of DD motor FE model.

Specification	Value
Number of slots	36
Number of poles	32
Length of air gap [mm]	1
Diameter of stator [mm]	222
Diameter of rotor [mm]	140
Number of coil turns	330
Coil winding	Distributed winding
Type of coil	Copper
Residual flux density [T]	1.3
Type of permanent magnet	Neodymium
Type of rotor	Iron
Type of stator	Electrical steel sheet

Figure 8 shows the results of the analysis of the continuous torque generated by the rotation of the rotor when a continuous current is applied. Figure 9 is a graph of the average value of the motor torque for each applied current. It shows the linear increase in the torque according to the increase in current. It was found to meet motor torque design specifications (above 35 Nm) by generating a torque of 39 Nm at a current of 6 A.

Table 4 shows the design specifications for building the actuator drive motor, reflecting the results of the DD motor design reviewed above. The DD motor is powered by three-phase 220 V and is expected to develop a torque of approximately 35 Nm or more when running at a rotational speed of 360 rpm with a current of 6 A.

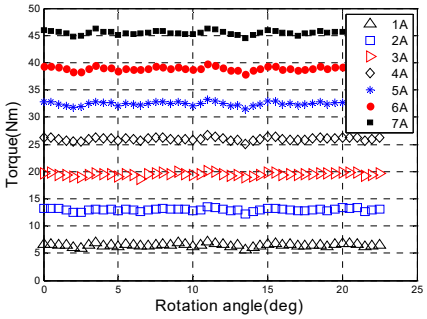


Figure 8. Continuous torque according to rotor rotation at continuous current.

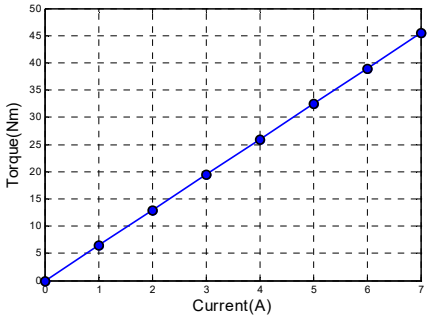


Figure 9. Torque variation according to the increase in current.

Table 4. Target specifications of the actuator's drive motor.

Item	Specification
Rated voltage	three-phase 220 VAC
Control type	three-phase PWM type
Rated current	6 A
Max. current	18 A
Rated torque	approx. 35 Nm
Max. torque	approx. 105 Nm
Max. RPM	above 360 rpm

3. Actuator Prototype

A prototype DD motor, the power source of the electro-mechanical actuator was manufactured. Figure 10 shows the shape of the DD motor prototype. In order to verify the torque performance of the DD motor prototype, the torque of the motor was tested using a torque tester as shown in Figure 11.

The speed of the motor was set to 360 rpm, which corresponds to the actuator's response speed of 0.3 Hz, and the torque was measured as the current changed. Figure 12 shows the results of the torque test with the prototype motor. When the magnitude of current is small, the difference between the design value and the test result is large due to the electric and mechanical resistance of the motor, but as the magnitude of current increases, the deviation decreases, so the target current of 6 A shows the torque performance that meets the design value. That is, the torque design value at a current of 6 A was 39.53 Nm, but the test result was 39.97 Nm, and the error was 1.1%. Therefore, it was judged that the torque performance of the developed DD motor meets the design target specifications. Please see Table 5 for detailed performance parameters.

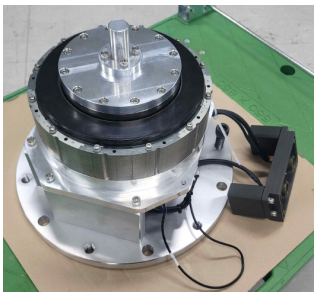


Figure 10. Prototype of the DD motor.

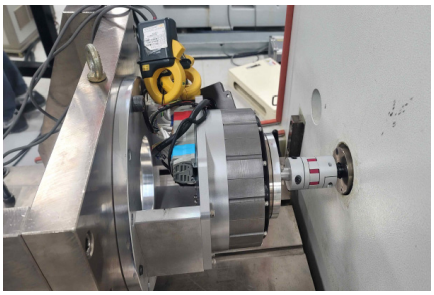


Figure 11. Torque test on the DD motor.

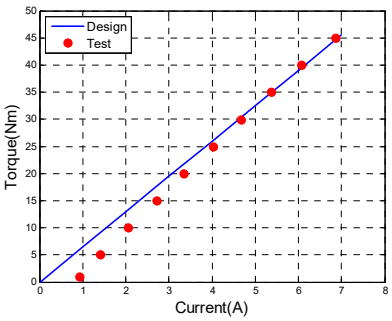


Figure 12. Torque test results for DD motor.

Table 5. Torque performance of the prototype of the DD motor.

Current (A)	Torque (Nm)		Error (%)
	Design	Test	
0.93	6.04	0.99	−83.6
1.41	9.16	5.03	−45.1
2.05	13.32	9.97	−25.2
2.71	17.61	15.00	−14.8
3.34	21.70	19.94	−8.1
4.02	26.12	24.99	−4.3
4.68	30.41	29.96	−1.5
5.37	34.90	34.98	0.2
6.08	39.53	39.97	1.1
6.87	44.67	44.98	0.7

Figure 13 shows an electro-mechanical actuator prototype mounted with a motor that has verified torque capability. The actuator prototype was tested to make sure that it met the actuator design specifications shown in Table 1. The test bench, shown in Figure 14, was built to test the actuator's maximum steering force of 50 kN. In order to measure the

steering force of the actuator, a reaction jig capable of holding up to about 80 kN of force was installed on the left and right sides of the actuator, and a load cell and a displacement sensor were installed to measure the steering force and stroke of the actuator.

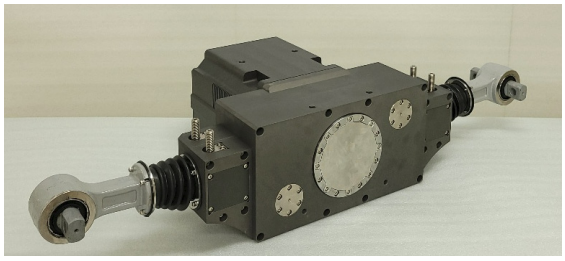


Figure 13. Prototype of the actuator.

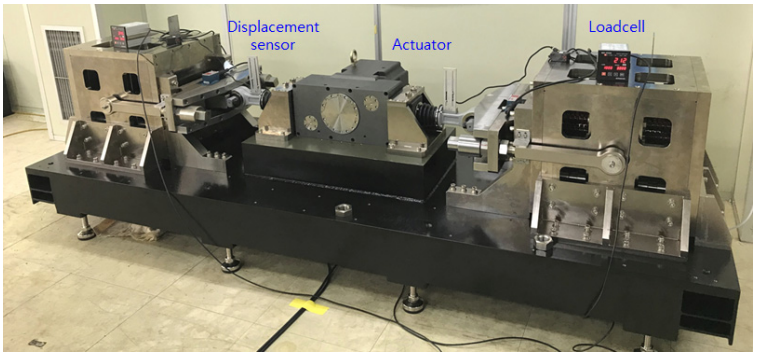


Figure 14. Test bench for testing the electro-mechanical actuator.

Figure 15 shows the test results for the stroke, steering force, and actuation frequency for the actuator prototypes tested using the test bench. The maximum performance that could meet all the stroke, steering force, and driving frequency target specifications was tested. In Figure 15a is the measured stroke data, which shows a maximum of 5.9 mm, exceeding the stroke development target specification of 5.5 mm. Figure 15b is the force measurement result measured at the end of the steering link. The maximum value is 54,909 N, which meets the actuator steering force target specification of 50,000 N or more. Figure 15c is the operating frequency of the actuator, with a measurement frequency of 0.32 Hz, exceeding the target specification of 0.3 Hz. Therefore, the developed electric mechanical actuator meets all the development target specifications, so it is thought that it can be used as a steering device when running a curved section of a railway vehicle.

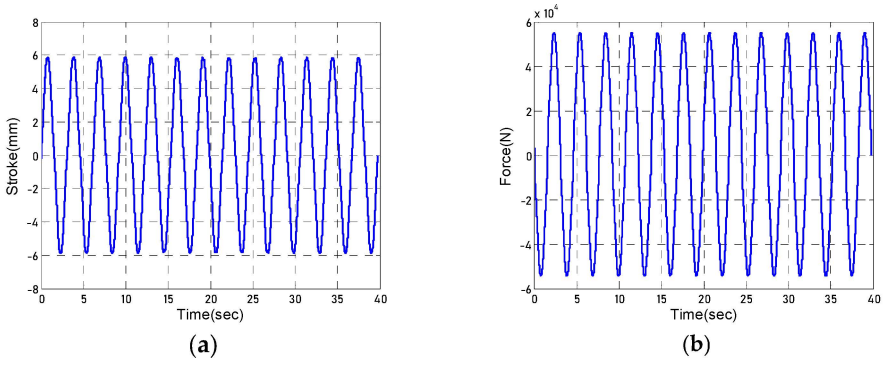
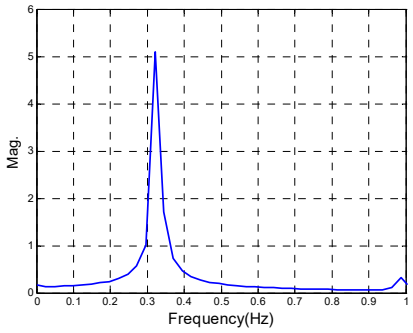


Figure 15. *Cont.*



(**c**)

Figure 15. Performance test results of the actuator using the test bench. (**a**) Stroke; (**b**) force; and (**c**) frequency.

4. Field Test

A field test was conducted by installing the developed electro-mechanical actuator prototype on a railway vehicle to verify its actual steering angle performance. A subway train operating on a commercial subway line with many curved sections was chosen as the test vehicle. To steer the wheelsets in the curved section, each steering actuator must be installed on the left and right sides of the bogie, which is the driving device of the railway vehicle, as shown in Figure 2. Therefore, as shown in Figure 16, two actuators were installed on both sides of the bogie. Figure 17 shows the shape of the bogie of the test train.

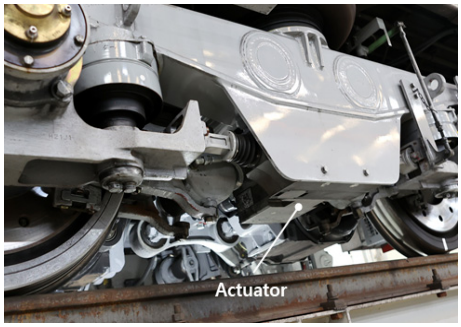


Figure 16. Steering actuator installed.



Figure 17. The bogie of the test train on bogie of the subway train.

The control for steering the wheelsets in the curved section is performed according to the steering control algorithm as shown in Figure 18. First, the curve is detected with a curve detection sensor, and the target steering angle is calculated as shown in Figure 4 by a steering controller. After that, the controller calculates the motor rotation angle of the steering actuator corresponding to the target steering angle and sends the command to the actuator motor to drive the actuator. The rotation angle of the motor actually driven

is measured by the encoder installed in the motor, and control is repeatedly performed to match the command motor rotation angle.

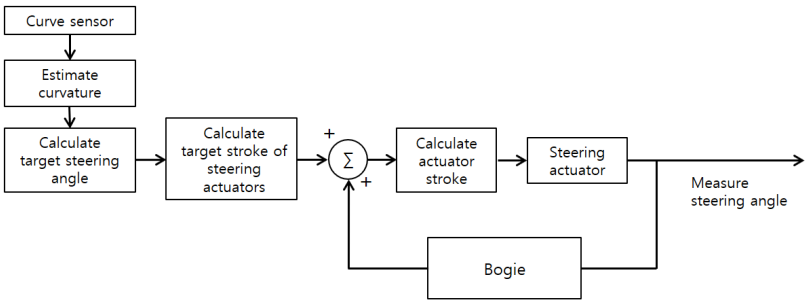


Figure 18. Block diagram for active steering control.

Figure 19 shows the curve distribution of the test line for the steering control test of the curved section. The total length of the test line is about 30 km, and various curves with different curved radii are distributed, and the curved radius of the minimum curve is 180 m. In the end, since it is important to measure the steering angle formed between the two wheelsets of the bogie by steering control while driving over the curved section, a cable type displacement sensor was installed as shown in Figure 20 to measure the distance between the two wheel sets.

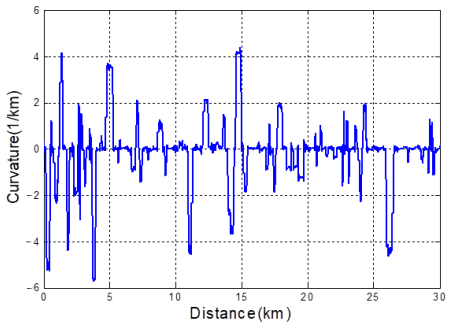


Figure 19. Curve distribution of the test line.

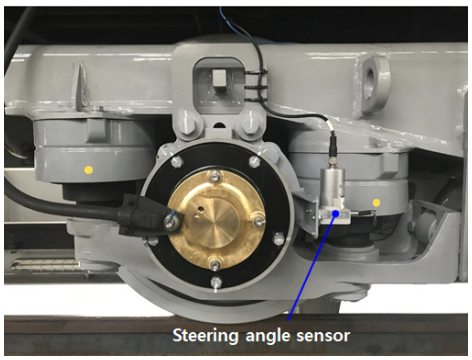


Figure 20. Steering angle sensor.

Figure 21 shows the displacement of the steering angle sensor measured during test line running. When driving on a curved section, as shown in Figure 19, the displacement of the left and right steering angle sensors occurs in the opposite phase due to the steering action. In other words, the spreading action between the axles required on the outer track causes positive displacements, while the pulling action required on the inner track causes negative displacements, leading to proper wheelset steering. The conversion of the displacement of this steering angle sensor to the steering angle is shown in Figure 22. It can be seen that the steering angle generated when passing through each curve meets the

target steering angle that can be implemented by the steering device. That is, the measured steering angles correspond with the target steering angles for a curve radius of 240 m or more, but are limited to 0.5 degrees for sharp curves with a radius of 240 m or less. The mean error between the measured steering angle and the target steering angle is only 3.4%, indicating that the steering action of the developed steering system is working very well. Therefore, the electro-mechanical actuator developed for application in the steering system of railway vehicles is judged to fully meet the actuator development specifications based on the laboratory and field test results mentioned above.

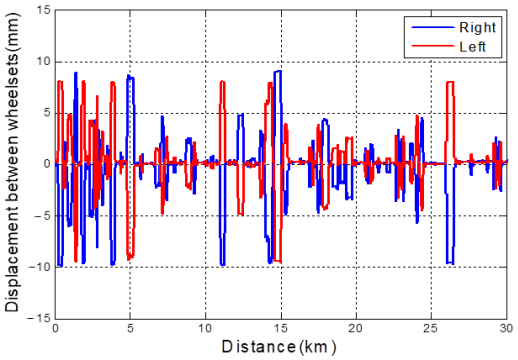


Figure 21. Measured displacement between wheelsets using the steering angle sensor.

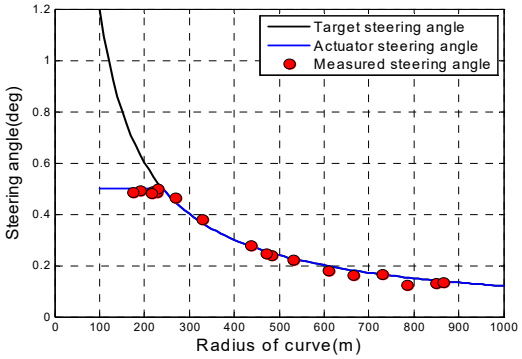


Figure 22. The steering angle measured from the field test.

5. Conclusions

In this paper, we developed an electro-mechanical steering actuator for use as a steering device for railway vehicles. This is the first time we have attempted to develop an electro-mechanical steering actuator, and specification derivation, design, prototyping, and testing have been carried out for the actuator.

We created specifications for the stoke, 5.5 mm, and for the steering force of a 50 kN-class electro-mechanical actuator capable of steering control for a railway curve radius of up to 250 m, and DD motor specifications were derived as a power source for driving it.

The DD motor was designed and the motor prototype was manufactured according to the proposed design.

We designed an electro-mechanical steering actuator and manufactured a prototype. We tested the actuator prototype using a test bench, and the stroke, steering force, and operating frequency each showed good performance exceeding the target specifications.

We conducted a field test on the actuator prototype by installing it on a railway vehicle to verify the steering angle performance. The steering action of the actuator worked well when running in curved sections, and the steering angles measured for each curve were in line with the target steering angles. The mean error between the target steering angle and the measured steering angle was only 3.4%, indicating that the wheel steering action of the developed steering system worked very well.

Therefore, the electro-mechanical steering actuator developed to steer the wheels of railway vehicles is expected to be fully utilized as a steering device for railway vehicles by meeting specifications and performance requirements.

Author Contributions: H.M.H. drew the actuator requirements and specifications, and J.H.C. made the motor. J.W.S. and K.H.M. were in charge of laboratory testing, while H.M.H. was in charge of field testing. All authors have read and agreed to the published version of the manuscript.

Funding: This paper was supported by the research funding of the Ministry of Land, Infrastructure and Transport's National Research and Development Project (Development of Technology for Commercialization of Active Steering Bogie for Electric Railway Vehicle in a Sharp Curve: KA163504).

Data Availability Statement: Data are contained within the article and shared by all authors.

Conflicts of Interest: Author J.H.C. is employee of Dodam Corporation. Other authors declare no conflicts of interest.

References

1. Pérez, J.; Busturia, J.M.; Goodall, R.M. Control strategies for active steering of bogie-based railway vehicles. *Control Eng. Pract.* **2002**, *10*, 1005–1012. [CrossRef]
2. Mei, T.X.; Goodall, R.M. Recent development in active steering of railway. *Veh. Syst. Dyn.* **2003**, *39*, 415–436. [CrossRef]
3. Fu, B.; Giossi, R.L.; Persson, R.; Stichel, S.; Bruni, S.; Goodall, R. Active suspension in railway vehicles: A literature survey. *Railw. Eng. Sci.* **2020**, *28*, 3–35. [CrossRef]
4. Liu, X.; Goodall, R.; Iwnicki, S. Yaw compensation and yaw relaxation controls for active steering of railway wheelsets via electromechanical actuators. *Proc. Inst. Mech. Eng. Part F J. Rail Rapid Transit* **2022**, *236*, 70–79. [CrossRef]
5. Sim, K.S.; Hur, H.M.; Song, H.S.; Park, T.W. Study of the Active Radial Steering of a Railway Vehicle using Curvature Measuring Method. *J. Mech. Sci. Technol.* **2014**, *28*, 4583–4591. [CrossRef]
6. Michálek, T.; Zelenka, J. Reduction of Lateral Forces between the Railway Vehicle and the Track in Small-Radius Curves by Means of Active Elements. *Appl. Comput. Mech.* **2011**, *5*, 187–196.
7. Umehara, Y.; Kamoshita, S.; Ishiguri, K.; Yamanaga, Y. Development of electro-hydraulic actuator with fail-safe function for steering system. *Q. Rep. RTRI* **2014**, *55*, 131–137. [CrossRef]
8. Suzuki, M.; Kodama, S.; Tanaka, T.; Umehara, Y.; Kamoshita, S.; Miyamoto, T. Evaluation of the performance of the bogie to control the decrement of wheel load using the test line of RTRI. *RTRI Rep.* **2016**, *30*, 17–22. [CrossRef] [PubMed]
9. Hur, H.M.; You, W.H.; Kim, M.S.; Park, J.H. Active Steering Control Apparatus for Railway Vehicles and the Method of the Same. Patent KR101084157B1, 16 November 2011.
10. Hur, H.M.; You, W.H.; Shin, Y.J.; Sim, K.S.; Park, T.W. Analysis on the Actuator Force of Active Steering Bogie for Radial Steering. In Proceedings of the KSPE Spring Conference, Seoul, Republic of Korea, 14–16 May 2014; Volume 99.

Disclaimer/Publisher's Note: The statements, opinions and data contained in all publications are solely those of the individual author(s) and contributor(s) and not of MDPI and/or the editor(s). MDPI and/or the editor(s) disclaim responsibility for any injury to people or property resulting from any ideas, methods, instructions or products referred to in the content.